Supplementary Information

Supplementary Figures

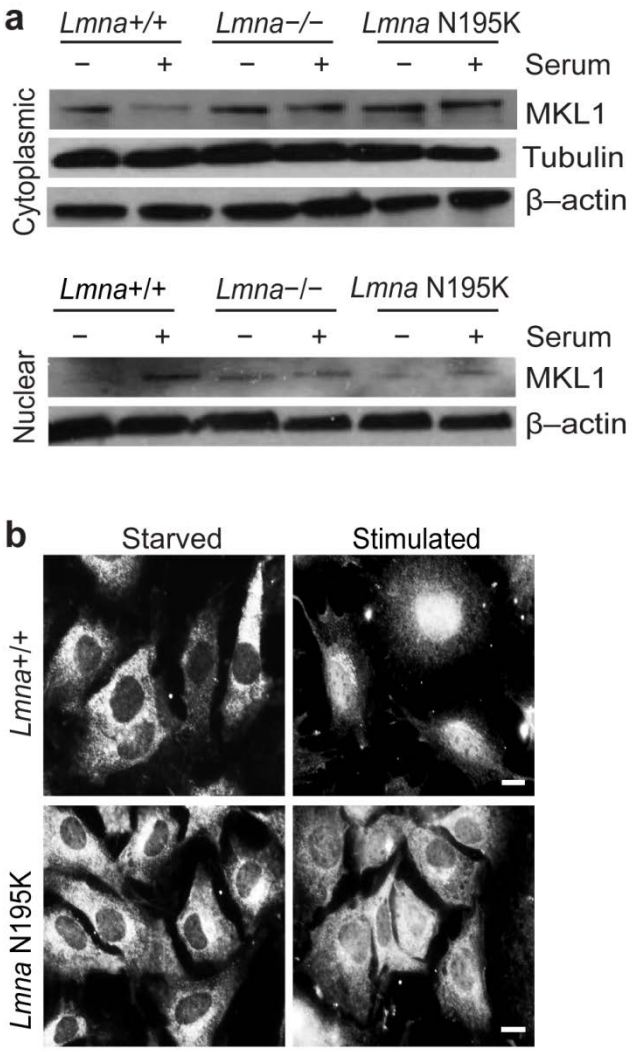

Supplementary Figure 1. Impaired nuclear translocation of MKL1 in lamin A/C-deficient and *Lmna* N195K mutant cells. (**a**) Cytoplasmic and nuclear extracts probed for MKL1 and β-actin and tubulin as loading controls. *Lmna*$^{+/+}$ cells show decreased cytoplasmic MKL1 and concomitant increase in nuclear MKL1 in response to serum stimulation, which is absent in *Lmna*$^{-/-}$ and *Lmna* N195K cells. (**b**) Representative images of *Lmna*$^{+/+}$ and *Lmna*$^{N195K/N195K}$ bone-marrow derived mouse mesenchymal stem cells immunofluorescently labeled for MKL1 before and after serum stimulation. Scale bar, 20 μm.

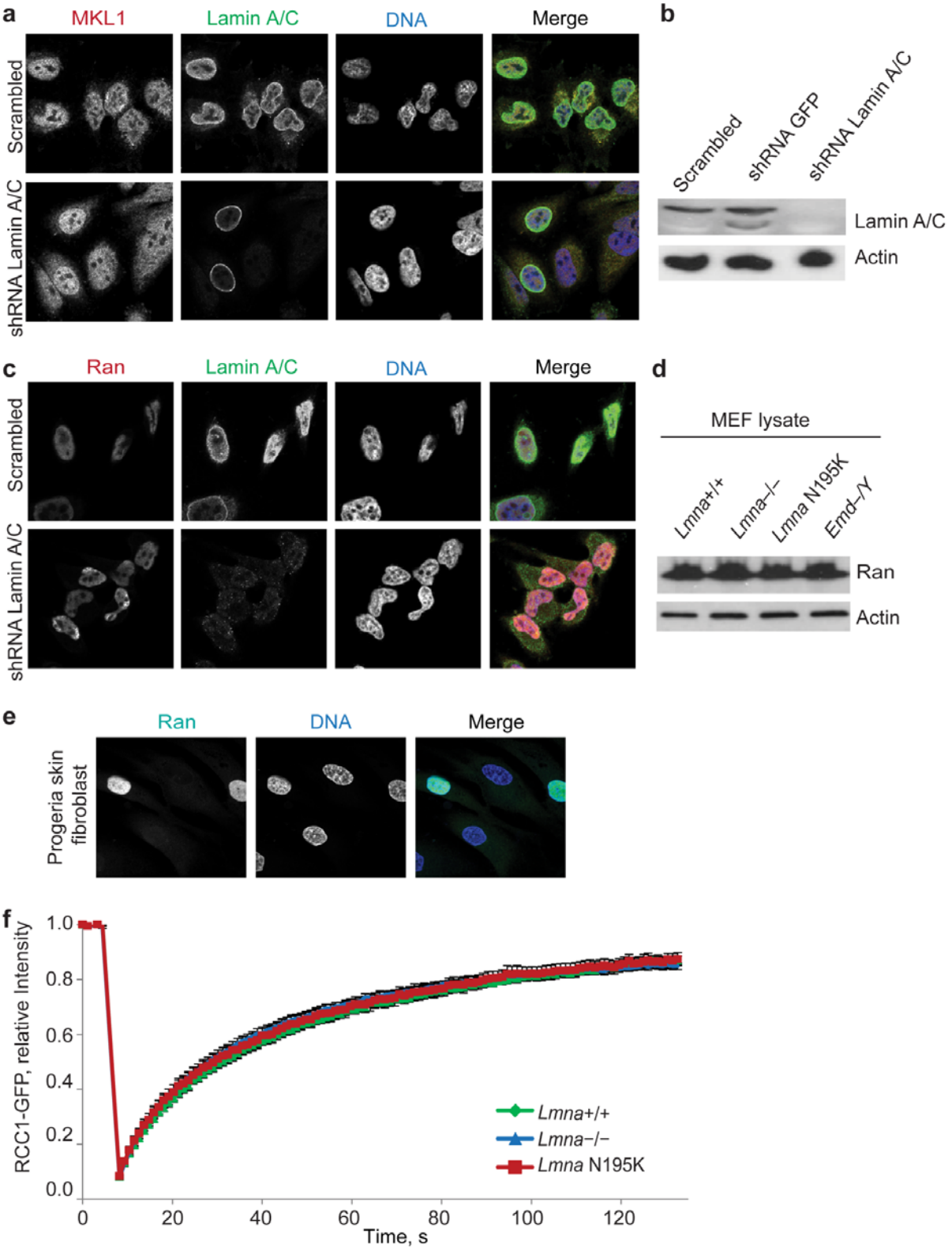

Supplementary Figure 2. Loss of lamins A/C impairs nuclear translocation of MKL1 but does not affect Ran protein localization and levels. (**a**) Representative images of serum-stimulated HeLa cells fluorescently labeled for lamins A/C and MKL1 after shRNA mediated knockdown of lamins A/C or scrambled control. The immunofluorescence images confirm lamin A/C knockdown and reduced nuclear accumulation of MKL1 upon serum stimulation in cells with reduced lamin A/C levels. In the merged images, DNA is shown in blue, lamin A/C in green and MKL1 in red. Scale bar, 10 μm. (**b**) Western blot analysis to confirm down-regulation of

lamin A/C in *Lmna* shRNA-treated HeLa cells and non-targeted controls. (**c**) Immunofluorescence analysis of lamin A/C and Ran in representative *Lmna* knockdown HeLa cells and non-targeted controls show that Ran localization is normal in these cells. DNA is shown in blue, lamin A/C in green, and Ran in red. Scale bar, 10 μm. (**d**) Representative Western analysis of Ran levels in $Lmna^{+/+}$, $Lmna^{-/-}$, *Lmna* N195K, and $Emd^{-/Y}$ cells. All cell lines had normal levels of Ran protein. (**e**) Since cells from HGPS patients have defects in the localization of the nuclear transport factor Ran,[1] we used HGPS patient fibroblasts as positive control for disturbed Ran localization. Unlike HGPS cells, however, $Lmna^{-/-}$ and *Lmna* N195K cells had normal Ran levels and localization. Representative immunofluorescence images showing defective Ran localization in a subpopulation of HGPS patient skin fibroblasts. Ran is shown in green and DNA is shown in blue. Scale bar, 10 μm. (**f**) Fluorescence recovery after photobleaching (FRAP) analysis of RCC1-GFP confirmed that $Lmna^{-/-}$ and *Lmna* N195K MEFs had normal mobility of RCC1. $N = 10$ for each cell line. Error bars, s.e.m.

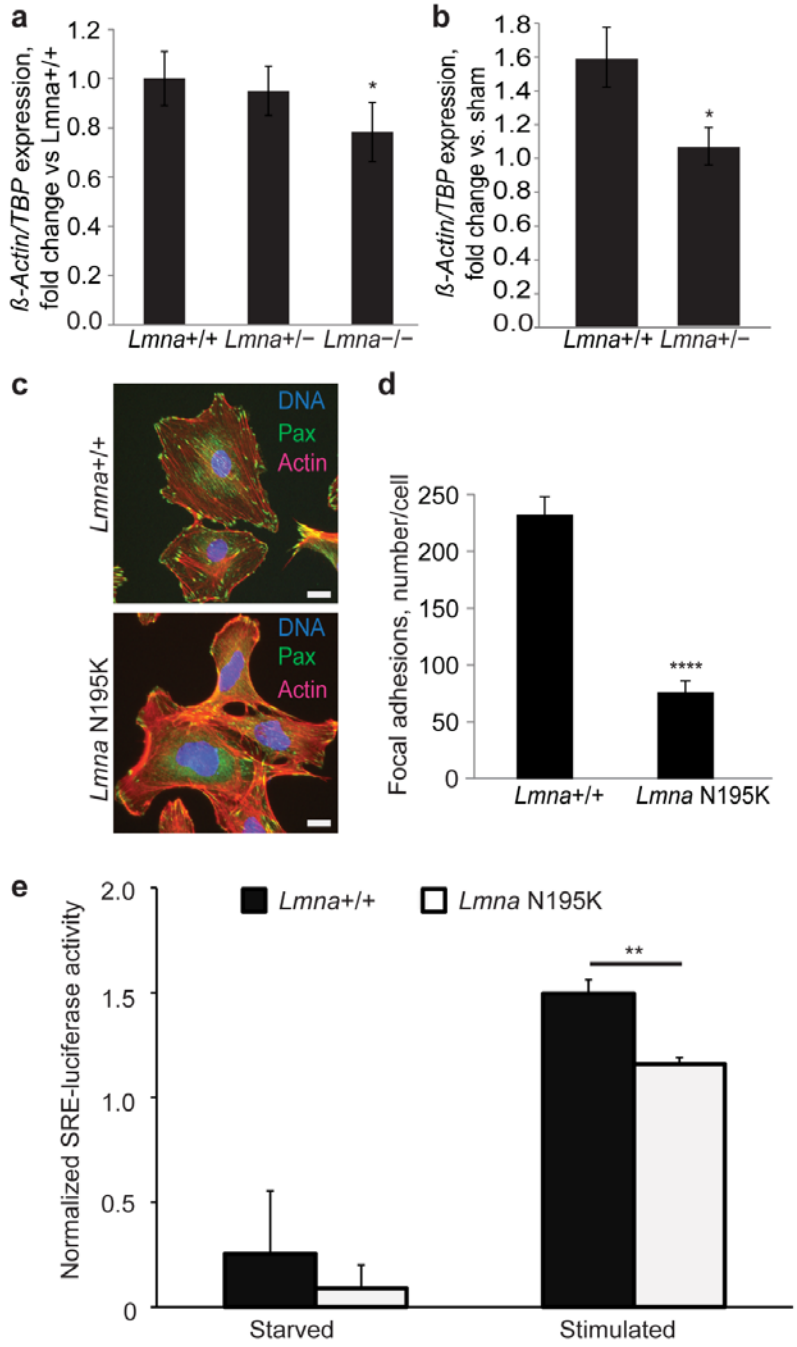

Supplementary Figure 3. Functional consequences of impaired MKL1 nuclear translocation (a) Gene expression of *β-Actin* in $Lmna^{+/+}$ (N = 9), $Lmna^{+/-}$ (N = 11) and $Lmna^{-/-}$ (N = 10) cardiac tissue. Values were normalized to *TBP*. (**b**) Gene expression of *β-Actin* in $Lmna^{+/+}$ (N = 5) and $Lmna^{+/-}$ (N = 7) cardiac tissue collected 1 week after transverse aortic constriction (TAC) surgery. Values were normalized to *TBP* and compared to those from sham animals. Statistical significance determined by Student's *t*-test, compared with $Lmna^{+/+}$ MEFs; *, indicates $P \leq 0.05$. (**c**) Immunofluorescence staining for F-actin and the focal adhesion protein paxillin in representative wild-type ($Lmna^{+/+}$) and *Lmna* N195K MEFs. DNA is shown in blue, actin in red, and paxillin in green. Scale bar, 20 µm. (**d**) *Lmna* N195K cells had fewer focal adhesions per cells than cells from wild-type ($Lmna^{+/+}$) littermates. (**e**) Serum response factor (SRF) promoter activity was lowered in *Lmna* N195K compared to $Lmna^{+/+}$ MEFs. SRF activity was quantified using a Dual-Glo Luciferase assay with serum response element (SRE)-luciferase. Values represent average of six biological replicates from two independent experiments. **, denotes $P \leq 0.01$ compared with corresponding $Lmna^{+/+}$ control. Error bars, s.e.m.

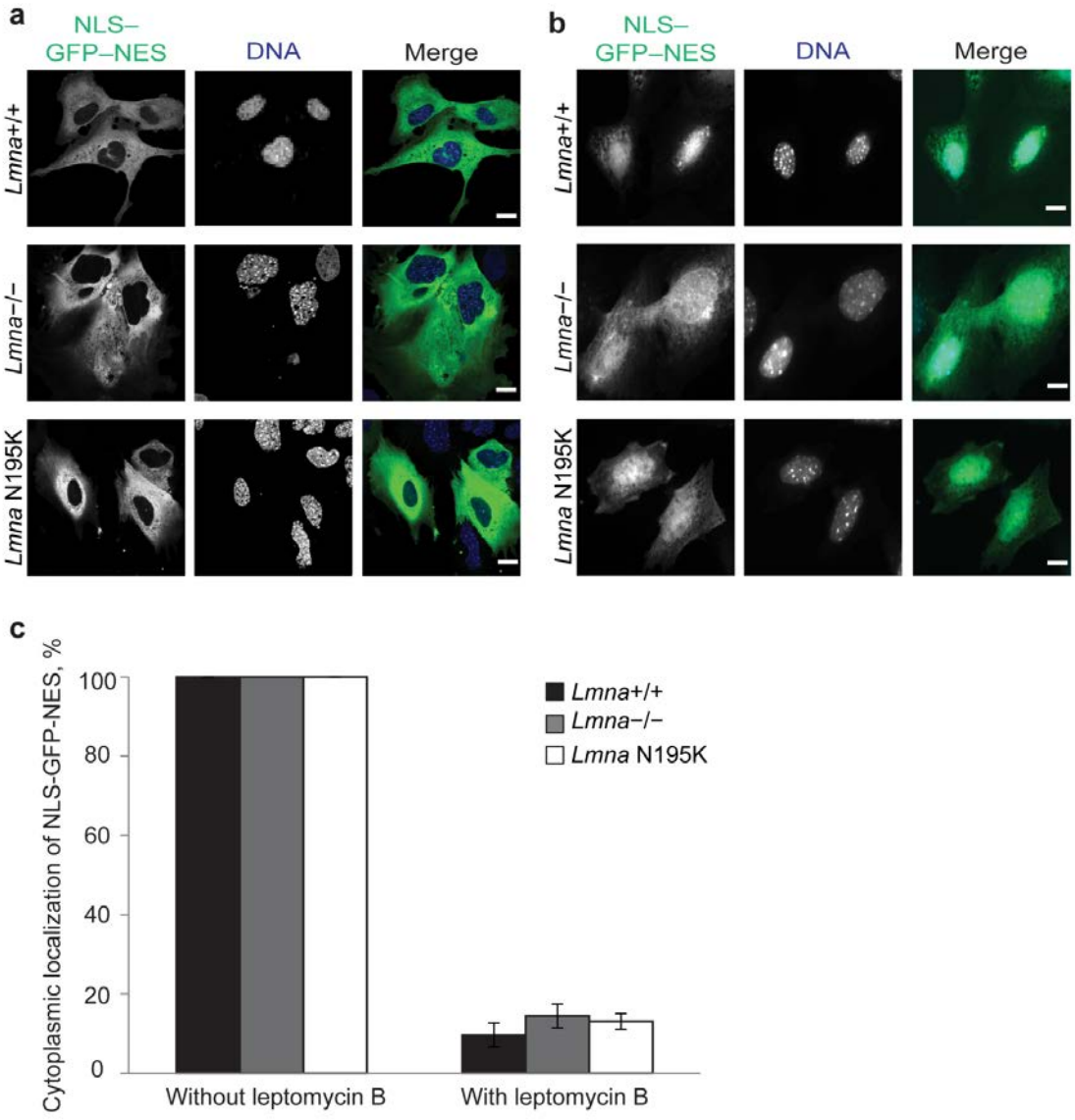

Supplementary Figure 4. Nuclear transport is generally preserved in the *Lmna*$^{-/-}$ and *Lmna* N195K cells. The NLS-GFP-NES reporter consisting of GFP fused to an NLS and a nuclear export sequence (NES). The SV40-derived NLS is importin α/β-dependent, similar to MKL1. Normally, the dominant NES drives cytoplasmic localization of the NLS-GFP-NES reporter; conversely, blocking nuclear export with leptomycin B results in nuclear accumulation of the reporter construct.[2] (**a**) Representative images of *Lmna*$^{+/+}$, *Lmna*$^{-/-}$ and *Lmna* N195K MEFs expressing the NLS-GFP-NES fusion construct. The NLS-GFP-NES was predominantly localized to the cytoplasm in all cell lines. DNA (Hoechst33342) is shown in blue; NLS-GFP-NES is shown in green. Scale bar, 20 μm. (**b**) *Lmna*$^{+/+}$, *Lmna*$^{-/-}$ and *Lmna* N195K MEFs expressing the NLS-GFP-NES construct treated with leptomycin B, a nuclear export inhibitor, resulting in accumulation of the NLS-GFP-NES reporter construct in the nucleus and indicating that general nuclear import is preserved in the *Lmna*$^{-/-}$ and *Lmna* N195K cells. DNA is shown in blue; NLS-GFP-NES is shown in green. Scale bar, 10 μm. (**c**) Quantification of cell fractions exhibiting cytoplasmic localization of the reporter construct, NLS-GFP-NES in the absence (left) and presence (right) of leptomycin B showed comparable levels of bulk import and export events. In the absence of leptomycin B, the NLS-GFP-NES showed completely cytoplasmic localization. In the presence of leptomycin B, only 9.7±3.07% (*Lmna*$^{+/+}$), 14.5±2.95% (*Lmna* $^{-/-}$) and 13.1±1.85% (*Lmna* N195K) cells exhibited cytoplasmic localization of this reporter. Data was expressed in percentage of cells with cytoplasmic localization of NLS-GFP-NES and was not significantly different among the 3 groups. $N \approx 100$ for each cell line. Error bars, s.e.m.

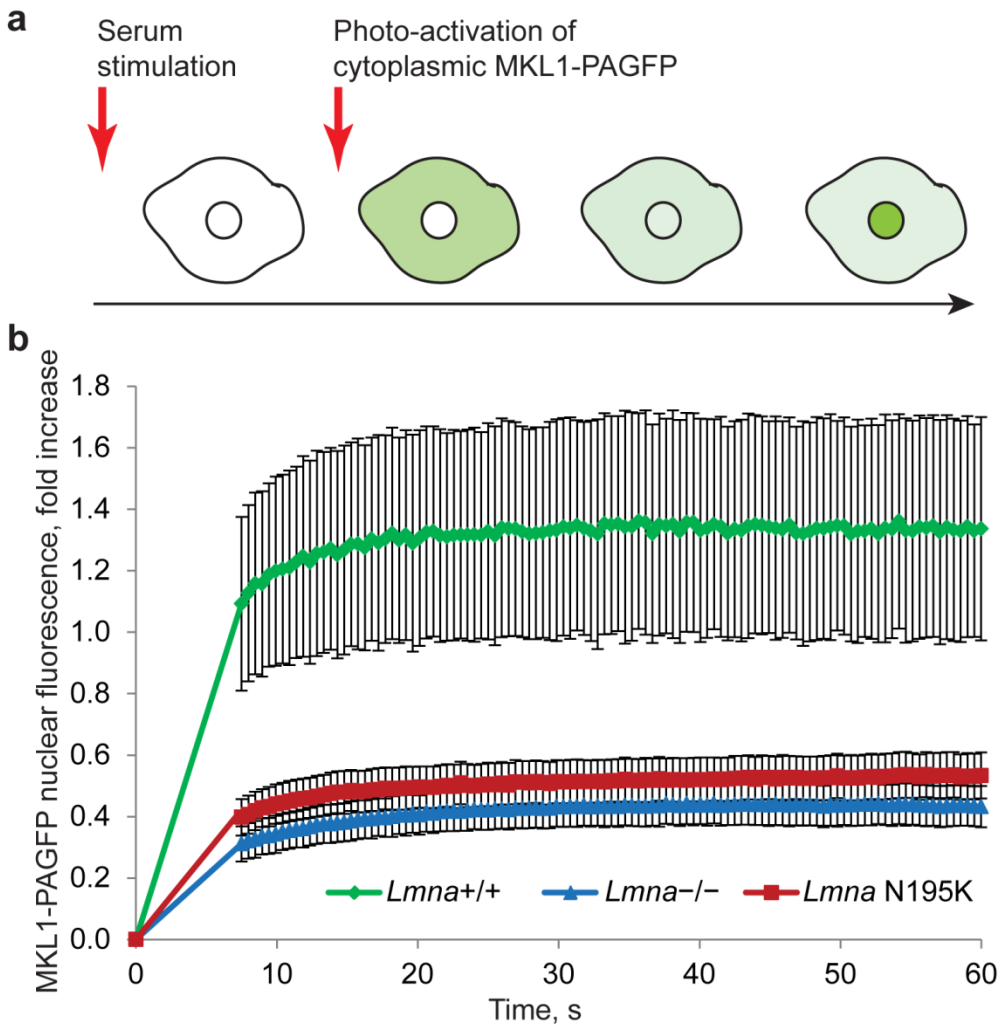

Supplementary Figure 5. Nuclear import of MKL1 is impaired in *Lmna*$^{-/-}$ and *Lmna* N195K cells. (**a**) Schematic diagram of experiments with cells expressing photoactivatable MKL1-GFP (MKL1-PAGFP) to measure nuclear import of MKL1. After serum stimulation, MKL1-PAGFP was selectively activated in the cytoplasm. Subsequent translocation of photoactivated MKL1-PAGFP into the nucleus was monitored by time-lapse confocal microscopy to reveal the rate of nuclear import. (**b**) The photoactivation experiments showed rapid entry and accumulation of activated cytoplasmic MKL1-PAGFP into the nucleus of *Lmna*$^{+/+}$ cells; in contrast, this response was significantly weaker in *Lmna*$^{-/-}$ and *Lmna* N195K MEFs. Nuclear fluorescence intensity of MKL1-PAGFP was normalized to the initial fluorescence of the cytoplasmic activation area. $N = 8$ for each cell line. Error bars, s.e.m.

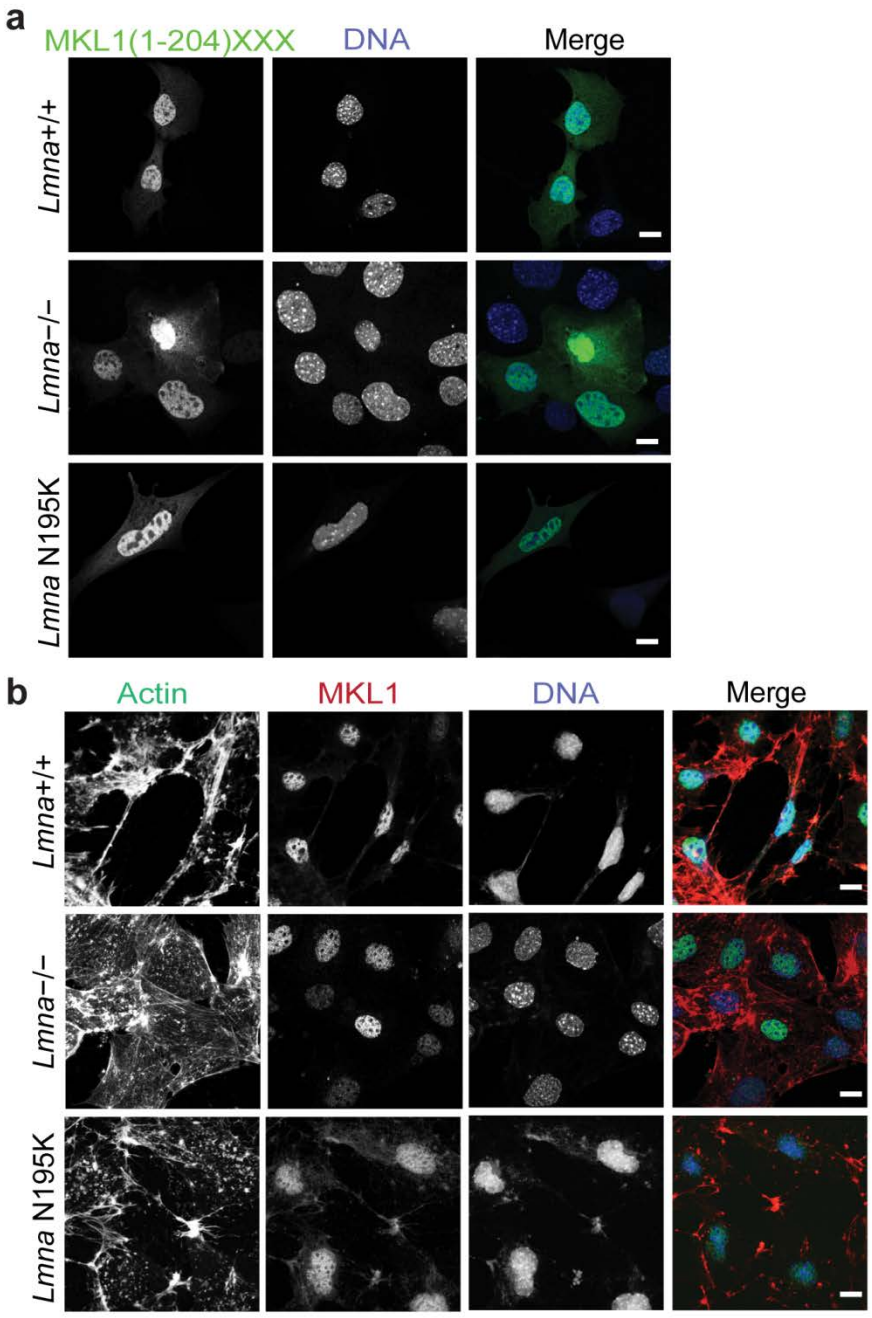

Supplementary Figure 6. Impaired nuclear translocation of MKL1 is caused by altered actin dynamics in *Lmna*$^{-/-}$ and *Lmna* N195K cells. (**a**) Fluorescence images of representative *Lmna*$^{+/+}$, *Lmna*$^{-/-}$ and *Lmna* N195K MEFs expressing a reporter construct (MKL1(1–204)XXX–2×GFP) similar to the MKL1(1–204)–2×GFP construct, but in which arginine-to-alanine substitution in all three RPEL domains of MKL1 prevent actin binding. MKL1(1–204)XXX–2×GFP localizes to the nucleus even in starved *Lmna*$^{+/+}$, *Lmna*$^{-/-}$ and *Lmna* N195K MEFs, indicating that MKL1 can enter the nucleus of *Lmna*$^{-/-}$ and *Lmna* N195K cells when decoupled from actin dynamics. DNA is shown in blue; MKL1(1–204)XXX–2×GFP in green. Scale bar, 10 µm. (**b**) Representative immunofluorescence images of endogenous MKL1 in *Lmna*$^{+/+}$, *Lmna*$^{-/-}$ and *Lmna* N195K MEFs treated with cytochalasin D, which disrupts the interaction between MKL1 and G-actin and results in nuclear translocation of MKL1 independent of actin dynamics in all cell lines. Scale bar, 10 µm.

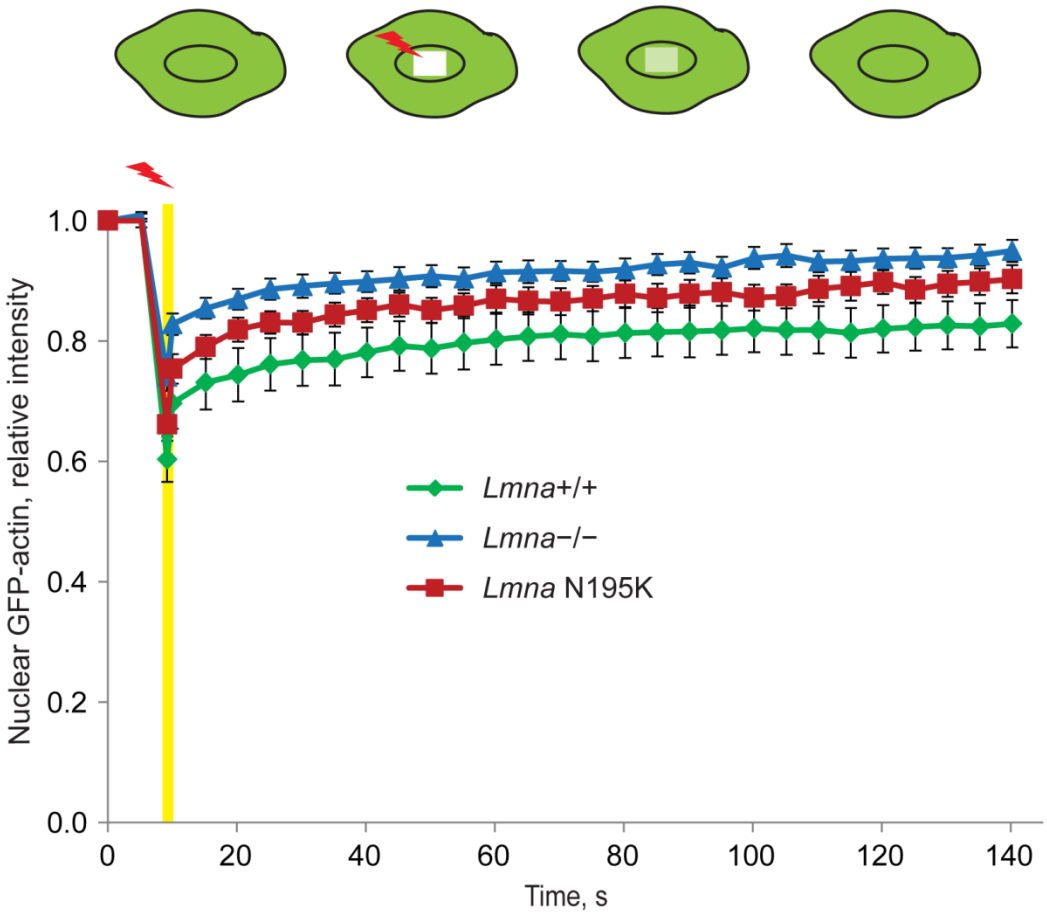

Supplementary Figure 7. *Lmna* mutant cells show increased nuclear actin mobility. Fluorescence recovery after photobleaching (FRAP) analysis of nuclear GFP-actin revealed increased actin mobility in *Lmna*$^{-/-}$ and *Lmna* N195K cells relative to *Lmna*$^{+/+}$ MEFs. *N* = 20 for each cell line. Error bars, s.e.m.

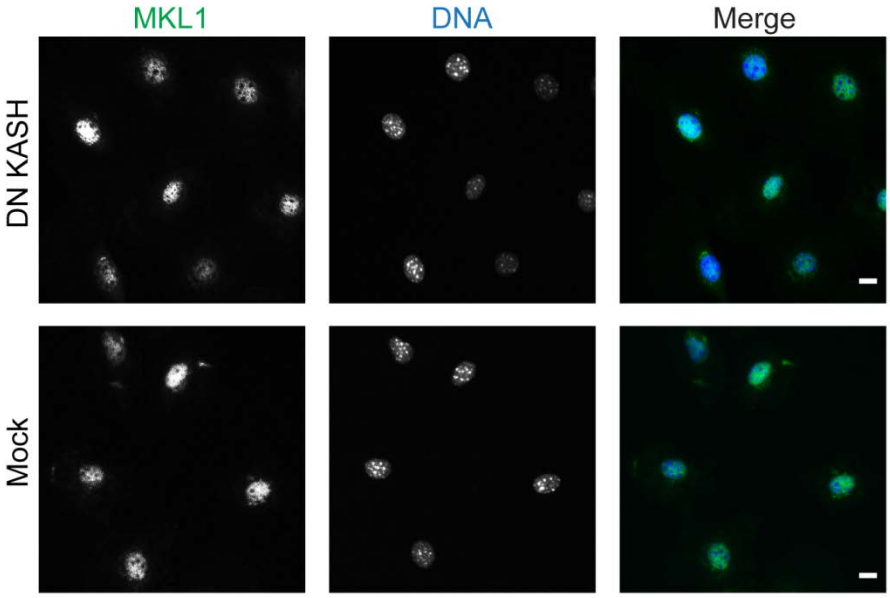

Supplementary Figure 8. MKL1 translocates normally into the nucleus in LINC complex-disrupted MEFs. Lamins A/C, together with nesprins and SUN proteins, are components of the LINC (linker of nucleoskeleton and cytoskeleton) complex that serves as a mechanical link between the nucleus and the cytoskeleton.[3] Cells were modified to express a dominant negative nesprin mutant (DN KASH) that displaces endogenous nesprins from the nuclear envelope and thus decouples the nucleus from the cytoskeleton,[4] similar to defects previously described in *Lmna*$^{-/-}$ MEFs.[5] Despite the obvious defects in nucleo-cytoskeletal coupling, DN KASH expressing cells had normal nuclear translocation of MKL1, consistent with a recent report that DN KASH modified cells have normal expression of vinculin in response to mechanical stimulation.[4] Shown are representative confocal immunofluorescence images of MKL1 localization in serum-stimulated MEFs expressing either DN-KASH or mock control. DNA is shown in blue. MKL1 is shown in green. Scale bar, 10 μm.

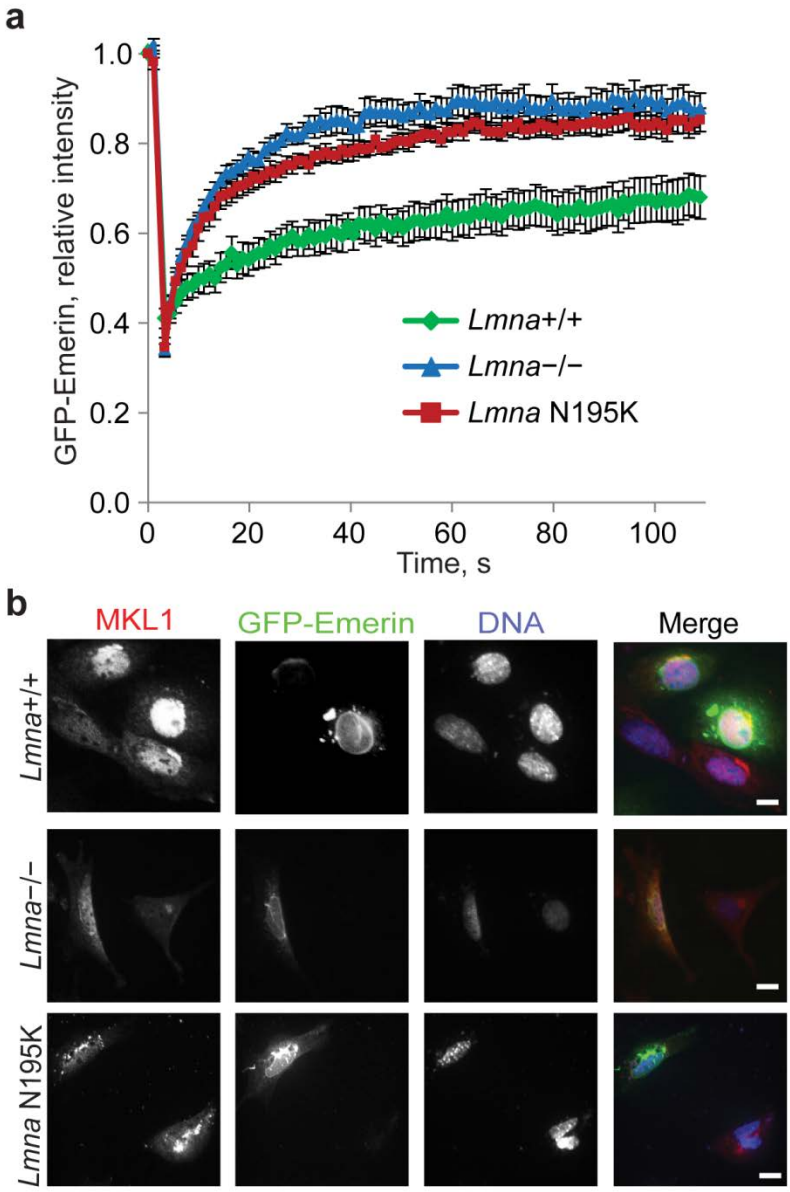

Supplementary Figure 9. Emerin expression restores MKL1 nuclear translocation in *Lmna*$^{-/-}$ and *Lmna* N195K cells. (**a**) Fluorescence recovery after photobleaching (FRAP) analysis revealed increased mobility of GFP-emerin at the nuclear envelope in *Lmna*$^{-/-}$ and *Lmna* N195K MEFs compared to *Lmna*$^{+/+}$ cells. $N = 10$ for each cell line. Error bars, s.e.m. (**b**) Representative images of MKL1 localization in cells transfected with GFP-emerin and stimulated with serum. Nuclear localization of MKL1 was restored in *Lmna*$^{-/-}$ and *Lmna* N195K cells expressing GFP-emerin. DNA is shown in blue, emerin in green, and MKL1 in red. Scale bar, 10 μm.

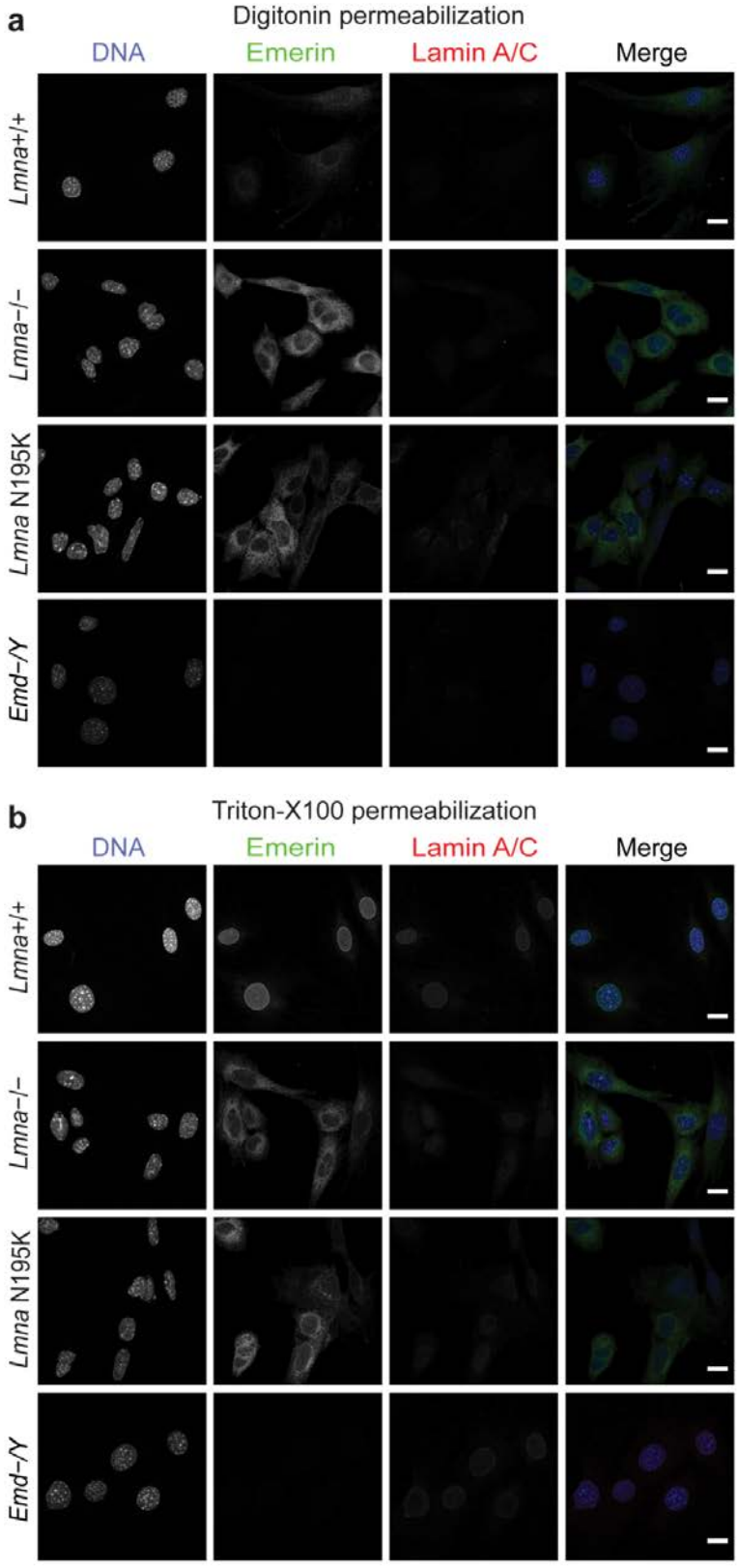

Supplementary Figure 10. A subset of emerin is located on the outer nuclear membrane and this fraction is increased in *Lmna* null and mutant cells. Digitonin-permeabilized cells stained for emerin (green) and lamin A/C (red) revealed that a fraction of emerin is localized to the outer nuclear membrane and endoplasmic reticulum in *Lmna*$^{+/+}$ MEFs. *Lmna*$^{-/-}$ and *Lmna* N195K cells displayed increased mislocalization of emerin in the outer nuclear membrane and endoplasmic reticulum. DNA is labeled in blue. Scale bar, 10 µm.

Descriptions for Supplementary Videos

Supplementary Movie 1. Nuclear translocation of MKL1-GFP in *Lmna*$^{+/+}$ MEFs. This movie shows an *Lmna*$^{+/+}$ mouse embryonic fibroblast expressing MKL1-GFP imaged before (frame 1) and immediately after serum stimulation (frames 2 and onwards). This time lapse covers a period of about 20 minutes. MKL1-GFP accumulated in the nucleus during the course of the movie. (QuickTime, 168 kb)

Supplementary Movie 2. Nuclear translocation of MKL1-GFP in *Lmna*$^{-/-}$ MEFs. This movie shows an *Lmna*$^{-/-}$ mouse embryonic fibroblast expressing MKL1-GFP imaged before (frame 1) and immediately after serum stimulation (frames 2 and onwards). This time lapse covers a period of about 20 minutes. Nuclear accumulation of MKL1-GFP is not evident during the course of the movie. (QuickTime, 428 kb)

Supplementary Movie 3. Nuclear translocation of MKL1-GFP in *Lmna* N195K MEFs. This movie shows an *Lmna* N195K mouse embryonic fibroblast expressing MKL1-GFP imaged before (frame 1) and immediately after serum stimulation (frames 2 and onwards). This time lapse covers a period of about 20 minutes. Nuclear accumulation of MKL1-GFP is not evident during the course of the movie. (QuickTime, 238 kb)

Supplementary Movie 4. Nuclear translocation of MKL1(1-204)- 2×GFP in *Lmna*$^{+/+}$ MEFs. This movie shows an *Lmna*$^{+/+}$ mouse embryonic fibroblast expressing MKL1(1-204)-2×GFP imaged before (frame 1) and immediately after serum stimulation (frames 2 and onwards). This time lapse covers a period of about 15 minutes. MKL1(1-204)-2×GFP accumulated rapidly in the nucleus during the course of the movie. (QuickTime, 178 kb)

Supplementary Movie 5. Nuclear translocation of MKL1(1-204)- 2×GFP in *Lmna*$^{-/-}$ MEFs. This movie shows an *Lmna*$^{-/-}$ mouse embryonic fibroblast expressing MKL1(1-204)-2×GFP imaged before (frame 1) and immediately after serum stimulation (frames 2 and onwards). This time lapse covers a period of about 15 minutes. Little or very low levels of MKL1(1-204)-2×GFP accumulated in the nucleus during the course of the movie. (QuickTime, 182 kb)

Supplementary Movie 6. Nuclear translocation of MKL1(1-204)- 2×GFP in *Lmna* N195K MEFs. This movie shows an *Lmna* N195K mouse embryonic fibroblast expressing MKL1(1-204)-2×GFP imaged before (frame 1) and immediately after serum stimulation (frames 2 and onwards). This time lapse covers a period of about 15 minutes. Little or very low levels of MKL1(1-204)-2×GFP accumulated in the nucleus during the course of the movie. (QuickTime, 191 kb)

Supplementary Movie 7. Photoactivation and nuclear translocation of MKL1-PAGFP in *Lmna*$^{+/+}$ MEFs. This movie shows an *Lmna*$^{+/+}$ mouse embryonic fibroblast (outlined in red) expressing MKL1-PAGFP after serum stimulation. Cytoplasmic MKL1-PAGFP was stimulated with a 405 nm laser and entry of the activated pool of MKL1-PAGFP is monitored for 1 minute. Frame 1 was captured before photoactivation. MKL1-PAGFP accumulated in the nucleus during the course of the movie. (QuickTime, 528 kb)

Supplementary Movie 8. Photoactivation and nuclear translocation of MKL1-PAGFP in *Lmna*$^{-/-}$ MEFs. This movie shows an *Lmna*$^{-/-}$ mouse embryonic fibroblast (outlined in red) expressing MKL1-PAGFP after serum stimulation. Cytoplasmic MKL1-PAGFP was stimulated with a 405 nm laser and entry of the activated pool of MKL1-PAGFP is monitored for 1 minute. Frame 1 was captured before photoactivation. MKL1-PAGFP did not accumulate in the nucleus during the course of the movie. (QuickTime, 387 kb)

Supplementary Movie 9. Photoactivation and nuclear translocation of MKL1-PAGFP in *Lmna* N195K MEFs. This movie shows an *Lmna* N195K mouse embryonic fibroblast (outlined in red) expressing MKL1-PAGFP after serum stimulation. Cytoplasmic MKL1-PAGFP was stimulated with a 405 nm laser and entry of

the activated pool of MKL1-PAGFP is monitored for 1 minute. Frame 1 was captured before photoactivation. MKL1-PAGFP did not accumulate in the nucleus during the course of the movie. (QuickTime, 490 kb)

References for Supplementary Materials

[1] Kelley, J. B. et al., The defective nuclear lamina in Hutchinson-gilford progeria syndrome disrupts the nucleocytoplasmic Ran gradient and inhibits nuclear localization of Ubc9. *Mol Cell Biol* **31** (16), 3378 (2011).

[2] Kudo, N. et al., Leptomycin B inhibition of signal-mediated nuclear export by direct binding to CRM1. *Exp Cell Res* **242** (2), 540 (1998).

[3] Wilson, K. L. and Foisner, R., Lamin-binding Proteins. *Cold Spring Harb Perspect Biol* **2** (4), a000554 (2010).

[4] Lombardi, M. L. and Lammerding, J., Keeping the LINC: the importance of nucleocytoskeletal coupling in intracellular force transmission and cellular function. *Biochem Soc Trans* **39** (6), 1729 (2011).

[5] Hale, C. M. et al., Dysfunctional connections between the nucleus and the actin and microtubule networks in laminopathic models. *Biophys J* **95** (11), 5462 (2008).